Heat transfer and pressure drop during evaporation and condensation of R134a inside microfin tubes of new design

LUIGI COLOMBO, *Assistant Professor, Dip. di Energetica, Politecnico di Milano, Italy.* luigi.colombo@polimi.it
ADRIANO MUZZIO, *Full Professor,* *Dip. di Energetica, Politecnico di Milano, Italy.* adriano.muzzio@polimi.it
ALFONSO NIRO, *Full Professor, Dip. di Energetica, Politecnico di Milano, Italy.* alfonso.niro@polimi.it

ABSTRACT

This paper reports on average heat transfer coefficients and pressure drops of oil-free R134a in flow-boiling and convective-condensation inside microfin tubes with a new cross-section profile. Data obtained for a smooth tube are also reported for comparison. All tubes have the same outside diameter of 9.52 mm; they are horizontally operated and are heated/cooled by a water stream. Both microfin tubes are characterized by sharp fins (apex angle of 40°) alternating with two different heights whereas the fin number is different, namely, 54 and 82, respectively. Evaporation tests are carried out at a nominal temperature of 5 °C, for a mass flow rate ranging from about 100 to 340 kg/(m^2s), inlet quality between 0.25 and 0.7, and quality change varying from 0.1 to 0.7, whereas for the condensation tests the nominal temperature is 35 °C, the mass flow rate varies between 100 and 440 kg/(m^2s), the inlet quality ranges from 0.75 to 0.1 and the quality change from 0.1 to 0.7. Finally, the paper presents comparisons between experimental data and estimates obtained by recent correlations specifically proposed for these tubes.

1. INTRODUCTION

Microfin tubes have outstanding performance in enhancing heat transfer for both evaporation and condensation and have been widely used in the air-conditioning and refrigeration industries. Thus, in recent years, many efforts have been spent in designing and developing microfin geometries which could provide high heat transfer coefficients and low pressure drop penalty.

Heat transfer characteristics of microfin tubes have been extensively studied over the past twenty years; detailed literature reviews are presented by (Webb 1993), (Webb 1994), (Thome 1994), (Kandlikar and Raykoff 1996) and (Schlager 1991). Several papers, focused on the effects of various geometrical parameters such as tube diameter, spiral angle, fin height and shape, spacing between the fins and the number of fins and proposed predictive correlations for both heat transfer and fluid-dynamics (Cavallini et al. 1998), (Cavallini et al. 2000), (Chamra et al. 2003). However, due to the complexity of the physical phemomena involved in fluid-dynamics and heat transfer, experimental research is still the most reliable approach to the study of the performances of new microfin tubes and refrigerants.

Moved by these reasons, we are currently performing an experimental investigation of flow boiling and convective condensation of halo-carbon refrigerants inside microfin tubes as described in (Muzzio et al. 1998). This paper reports on average heat transfer coefficient and pressure drop during evaporation and condensation of oil-free refrigerant R134a in a smooth tube and two microfin tubes with new cross-section profiles. The main difference between microfin tubes consists in the number of fins so that, from the comparison of the performance, the effect of this parameter can be inferred. All the tubes have the same outer diameter of 9.52 mm and are horizontally operated.

2. APPARATUS AND TEST PROCEDURE

The experimental equipment was described in some detail in a previous paper by (Muzzio et al. 1998) and will, therefore, be covered only briefly here. A simplified schematic diagram of the experimental facility is shown in Figure 1. The rig consists of three circuits, namely, a sealed refrigerant circuit, a water circuit to evaporate or condense the refrigerant in the test section, and a chilled coolant (water-glycol solution) circuit.

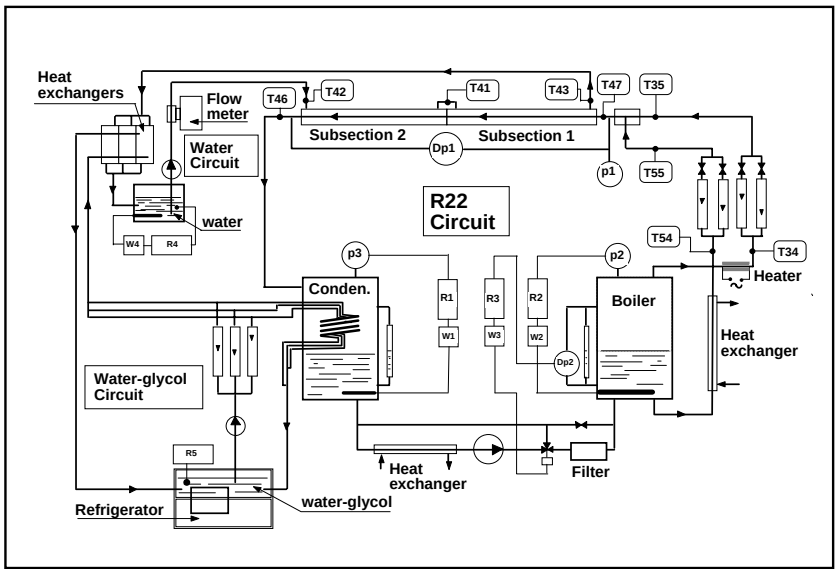

Figure 1. Schematic diagram of the experimental facility.

The main components of the refrigerant circuit are a boiler, the test section, a condenser, a gear pump and a filter dryer. The boiler is equipped with a heater consisting of three electrical cartridges of 1, 1.5 and 2.5 kW power. Liquid and vapour are drawn from it through two distinct lines; the liquid line is equipped with a subcooler, while a superheater is installed on the vapour line. The liquid mass flow rate is measured by a Coriolis flow meter, while float-type flow meters are installed on the vapour line. The liquid and vapour flow rates are controlled by precision metering valves. Downstream of the valves, vapour and liquid streams are mixed; the resulting two-phase mixture flows through a 1.5 m long calming section and then enters the test section. At the exit, refrigerant flows through a second calming section (1.8 m) and then is discharged to the condenser, which maintains the test section outlet pressure at a given value. Finally, the refrigerant is drawn from the condenser by a gear pump and is conveyed through a filter dryer to the boiler.

The water loop sets the condition of the water entering the annulus side of the test section. It contains a centrifugal pump that circulates demineralized water, a magnetic flow meter that measures the flow rate, and a combination of a plate heat exchanger and an electrical heater controlling the water temperature. Finally, the chilled coolant circuit is filled with a water-glycol solution and it consists of a commercial refrigeration unit and a centrifugal pump. Such a circuit provides the cold medium circulating in the heat exchangers placed in the refrigerant condenser or mounted on both the refrigerant and the water circuits.

The test section contains the tube undergoing experimental testing. It consists of a double-pipe heat exchanger, divided into two identical subsections, where refrigerant flows inside the inner tube and water flows counter-currently in the outer annulus. The inner tube is made of copper with 9.52 mm o.d. and 1.3 m length. The distance between the inlet and discharge ducts of the jacket is 1.12 m which is assumed as the active heat transfer length for the subsection. At the exit of both subsections a sight glass made of 80 mm long, 8.5 mm i.d., pyrex smooth tube is mounted. These sight glasses are neither heated nor cooled. Two pressure-taps are located at the inlet and outlet of the first subsection and at the outlet of the second one, respectively. Both subsections are equipped with four T-type thermocouples to measure wall temperatures. The thermocouples are placed in pairs on the top and at the bottom of the tube and are cemented in longitudinal grooves cut in the outside wall of

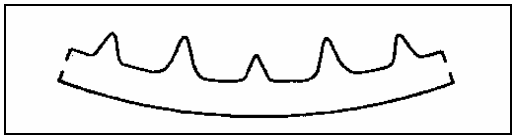

Figure 2. Cross sectional profile of the microfin tube

Parameter	VA	HVA	smooth
Outside diameter [mm]	9.52	9.52	9.52
Maximum inside diameter [mm]	8.92	8.62	8.92
Bottom wall thickness [mm]	0.30	0.45	0.30
Higher fin height [mm]	0.23	0.20	-
Lower fin height [mm]	0.16	0.17	-
Apex angle	40°	40°	-
Number of grooves	54	82	-
Helix angle	18°	18°	-
Inside-surface area ratio	1.58	1.84	1
Actual cross-section area ratio	0.96	0.95	1

Table 1. Geometrical parameters of the tested tubes.

the tube. Calming and test sections are thermally insulated by a 10 cm thick, glass-wool annulus.

Signals from thermocouples and transducers are cyclically read by a data acquisition unit and sent to an on-line PC. In order for all variables to be affected by similar RMS relative errors, the measurements of refrigerant temperature, pressure drop and water flow rate are based on 30, 50 and 100 readings for cycle, respectively. Every experimental datum, instead, is obtained by averaging the measurements of ten cycles in order to reduce the influence of random errors and fluctuations. Finally, for every operating condition, more than ten experimental data are collected.

The heat transfer coefficient is computed as follows. We assume that the refrigerant temperature varies linearly between the value T_{in}, measured at the entrance of the test section, and the value T_{out} computed at the exit as $T_s(p_s(T_{in})-\Delta p)$, where T_s is the function correlating the saturation temperature to the pressure, p_s the inverse function of T_s, and Δp the pressure drop measured along the test section. Then, for each subsection we calculate the mean refrigerant temperature $T_{r.m,i}$, the mean wall temperature $T_{w.m,i}$, the refrigerant to wall temperature mean difference $\Delta T_{m,i} = (T_{w.m,i}-T_{r.m,i})$, and the heat transfer coefficient $h_i=q_i/\Delta T_{m,i}$ where q_i is the mean heat flux based on a nominal inside area corresponding to the maximum internal diameter, i.e, the diameter at the root of microfins. Eventually, we compute the average heat transfer coefficient for the test section as the arithmetic mean of the subsection coefficients h_i. Relevant variables for the present investigation are affected by the following representative experimental uncertainties measured or estimated by a propagation error analysis: ±2.8% for the refrigerant mass flow rate, ±1.3% for the inlet quality, ±0.2 K between the refrigerant temperature and the saturation one, ±0.03 K between the wall and refrigerant temperatures with the refrigerant trapped in the test section and the water flowing, ±1.0% for the refrigerant pressure drop, ±1.0% for the water volume flow rate, ±0.02 K for the water temperature difference between the subsection inlet and outlet, ±1.4% for the heat rate, and ±7% for the average heat transfer coefficient.

3. RESULTS AND DISCUSSION

In saturated flow boiling or convective condensation, for fixed test section configuration, i.e., dimension and shape of the cross section, length, orientation with respect to gravity, both pressure drop and average heat transfer coefficient depend on four independent variables, namely, total mass flow rate, temperature (or pressure), inlet thermodynamic quality and heat rate. Since quality change along the test section depends linearly on heat rate, a different but equivalent parameterisation can be obtained by substituting the former with the latter quantity in the list of independent variables.

The experimental data reported here were obtained on two microfin tubes of new design developed and manufactured by Trefimetaux, i.e., Metofin 952-30VA40/54A and 952-45HVA 40/82, as well as on a smooth tube. All tubes have the same outer diameter of 9.52 mm. The microfin tubes tested, which we will denote as tubes VA and HVA respectively, are both characterized by sharp fins (apex angle of 40°) alternating with two different heights. This latter feature distinguishes these tubes from other microfin tubes of new design. A cross-section drawing of the tubes VA and HVA, whose main distinction lies in the fin numbers, is reported in Figure 2, whereas values of their geometric parameters are listed in Table 1 together with dimensions of the smooth tube. This table also lists the heat transfer internal surface ratio and the actual cross-section ratio with respect to the smooth tube.

Evaporation tests were carried out only on the HVA tube, because of time constraints, at a nominal saturation

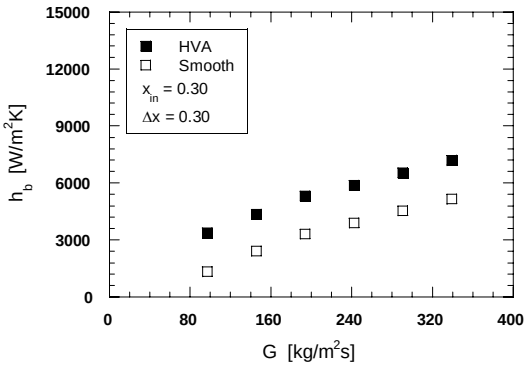

Figure 3. Flow-boiling coefficient h_b versus mass flux G for fixed inlet quality x_{in} and quality change Δx.

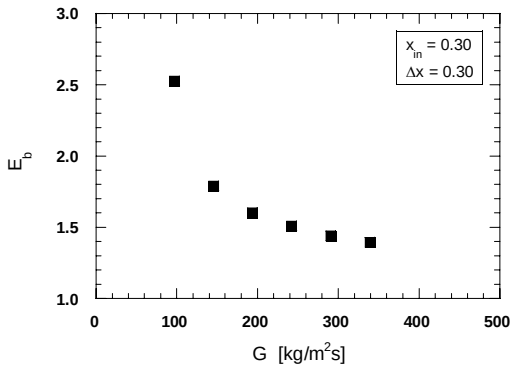

Figure 4. Enhancement factor versus mass flux G for fixed inlet quality x_{in} and quality change Δx.

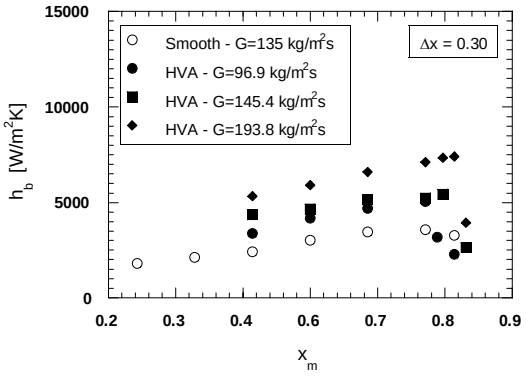

Figure 5. Flow-boiling coefficient h_b versus average quality x_m for fixed mass flux G and quality change Δx.

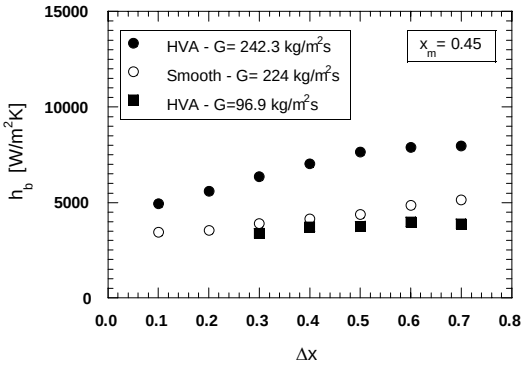

Figure 6. Flow-boiling coefficient h_b versus quality change Δx for fixed mass flux G and average quality x_m.

temperature of 5 °C (±0.2 K) corresponding to a pressure of 0.35 Mpa, while, in condensation, the nominal temperature was 35 °C (±0.2 K) corresponding to a pressure of 0.887 MPa. Total mass flow rate, inlet thermodynamic quality and quality change were varied in turn while keeping the others constant, in order to demonstrate clearly the effect of each variable against the others. The total mass flow rate ranged from 5.56 to 19.45 g/s corresponding to a mass flux G, with respect to a nominal cross-section area based on the maximum internal diameter, varying between about 100 and 340 kg/(m^{2}s) in evaporation. In condensation, the range of the total mass flow rate was from 5.56 to 25 g/s, corresponding to a mass flux G between about 100 and 440 kg/(m^{2}s). The inlet quality x_{in} was varied from 0.25 to 0.70 in evaporation, and between 0.75 and 0.1 in condensation; the quality change Δx from 0.1 to 0.7 in evaporation and from 0.1 to 0.7 in condensation.

Figure 3 shows the boiling heat transfer coefficient h_b plotted versus the mass flux G for the tested microfin tube HVA; data obtained on the smooth tube are also included for comparison. For such data, nominal inlet quality and quality change are x_{in}=0.3 and Δx=0.3, respectively. In considering this figure it is worth keeping in mind that as the mass flux increases at constant Δx an accompanying variation in heat flux sets up. For the data here reported, the average heat flux ranges from between 5.1 and 17.8 kW/m^2.

As expected, the boiling heat transfer coefficient is an increasing function of G, and its values for the microfin tube result higher than that for the smooth tube. Differences in thermal performances are well accounted by the enhancement factor E_b, depicted in Figure 4. It is a decreasing function of the mass flow rate and it seems to tend asymptotically to about 1.4, that is, a value smaller than the internal surface ratio. These results do not conform to the remark by (Eckels and Pate 1992) who, on the basis of the findings of their experimental studies, concluded that at high mass flux, the heat transfer increase in the microfin tube is due to the area increase. On the contrary, even at high mass flux, they support the observation by (Ito and Kimura 1979) that the increase in boiling heat transfer coefficient cannot be explained simply on the basis of area extension.

The effect of average quality x_m on the evaporation heat transfer coefficient, for fixed mass flux and quality change (Δx=0.3), is shown in Figure 5. For the microfin tube, a distinct maximum in heat transfer coefficient is observed at high average vapour quality, ranging from about 0.75 to 0.8. The corresponding value of x_m seems to increase slightly with the mass flux. This behaviour may be attributed to the transition from stratified-wavy flow, where the major heat transfer mechanism may be due to nucleate boiling, to annular flow, where forced

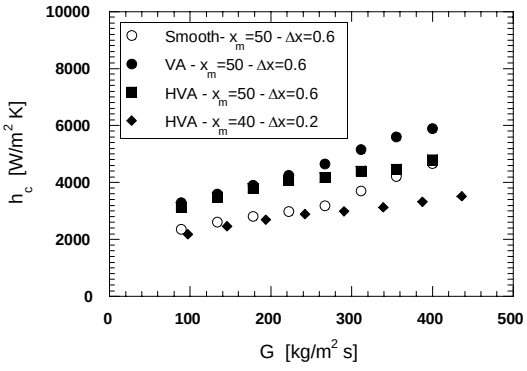

Figure 7. Heat transfer coefficient h_c versus mass flux G for fixed inlet quality xin and quality change Δx.

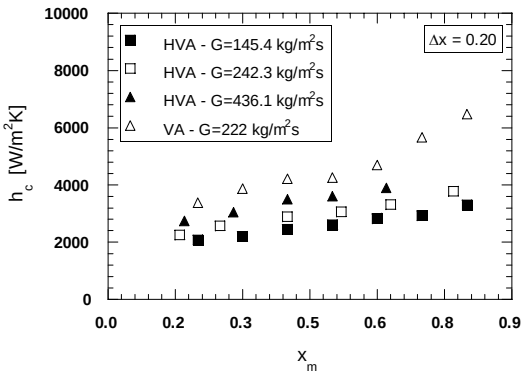

Figure 8. Heat transfer coefficient h_c versus average quality x_m for fixed mass flux G and quality change Δx.

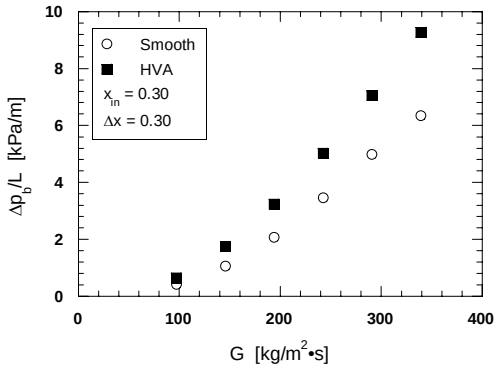

Figure 9. Flow-boiling pressure drop $\Delta p_b/L$ versus mass flux G for fixed inlet quality x_{in} and quality change Δx.

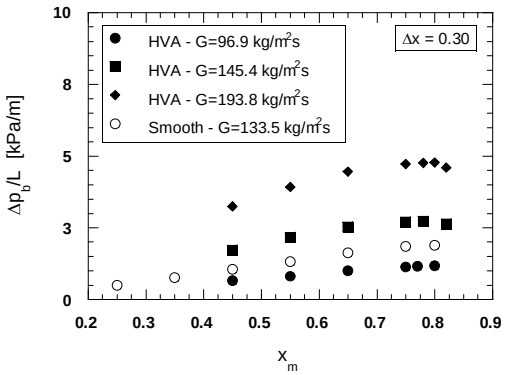

Figure 10. Flow-boiling pressure drop $\Delta p_b/L$ versus average quality x_m for fixed mass flux G and quality change Δx.

convection heat transfer is dominant. The preceding remarks are supported by the visual observation of the flow patterns, that showed a shift toward lower vapour qualities of the flow regime transition with increasing mass flux. The fall off in the heat transfer coefficient after the peak is caused by the dryout onset. In fact, heat transfer data relevant to the second subsection, not reported here, indicate that dryout occurs at a vapour quality of approximately 0.9.

For the smooth tube, instead, a slightly marked maximum, located approximately at x_m=0.7, is observed. The comparison between the data for the HVA tube at G=145.4 kg/(m^{2}s) and those for the smooth one at about the same mass flux shows that microfinning seems to provide, in addition to the substantial heat transfer enhancement, a shift of the dryout occurrence in the region of higher qualities. Besides, the heat transfer augmentation decreases with increasing vapour quality.

The influence of the quality change (heat flux) for given mass flux and average quality x_m=0.45 is depicted in Figure 6. We see that the heat transfer coefficient is not strongly affected by the quality change at G=96.9 kg/(m^{2}s). However, for G=242.3 kg/(m^{2}s) it may be noted that h_b is an increasing function of quality variation, up to $\Delta x \cong 0.5$; then the rise lowers and the trend seems to flatten. Instead the smooth channel at about the same mass flux exhibits a weak increase of the heat transfer coefficient with quality variation.

Attention may now be turned to condensation. Figure 7 displays the average heat transfer coefficient h_c plotted versus the mass flux G for the microfin and smooth tubes. In considering this figure, it is worth noting that mass flux variations at constant Δx imply proportional variations in heat flux due to their linear dependence; for the data here reported, the average heat flux ranges from 1.5 to 13.2 kW/m^2. As expected, the heat transfer coefficient is an increasing function of G, but trend for the microfin tubes differs from that of the smooth tube. For the latter, data exhibit a linear-at-interval dependence on G with a change of slope approximately at G=250 kg/(m^{2}s). Supported by visual observations, we infer that in the first region, where heat transfer is weakly dependent on the mass flux, the flow is stratified whereas it is annular when h_c starts to increase more steeply with G. Both the microfin tubes exhibit higher values of heat transfer coefficient and data do not display any change of slope marking the transition from stratified to annular flow. Results qualitatively similar to those reported in Figure 7 have been obtained for quality changes of 0.2 and 0.4, as can be observed from the data for the HVA tube at x_m=0.4 and Δx=0.2.

Differences in thermal performances are well accounted by the enhancement factor. For the VA-tube the enhancement factor varies within 1.5 and 1.25; hence, the enhancement factor remains lower than the inside-surface area ratio of this tube that amounts to 1.58. Data for the HVA-tube show that the enhancement factor is in the range from 1 to 1.38; therefore, for this microfin tube, discrepancy between heat transfer enhancement and area increase, that amounts to 1.84, becomes relevant. Since the VA- and HVA-tubes have quite similar geometries which essentially differ only in the fin number, we infer that a large number of fins decreases the enhancement in condensation, in accordance with the findings of (Yasuda et al. 1990); moreover, geometry can affect negatively fluid dynamics and heat transfer. Finally, from the thermal standpoint, the data clearly show the superiority of the VA geometry with respect to the HVA geometry.

Figure 8 depicts the effect of the average quality on the condensation heat transfer coefficient. It is seen that h_c increases with quality at constant mass flux and quality change. In particular, when comparing the two

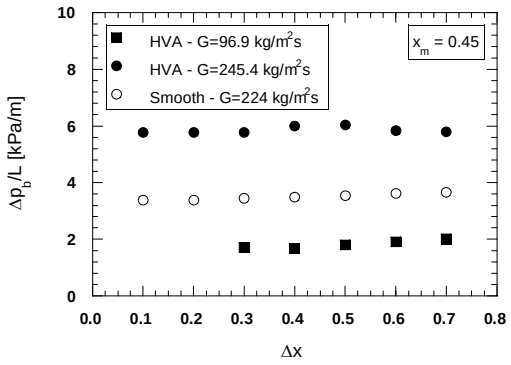

Figure 11. Flow-boiling pressure drop $\Delta p_b/L$ versus quality change Δx for fixed mass flux G and average quality x_m.

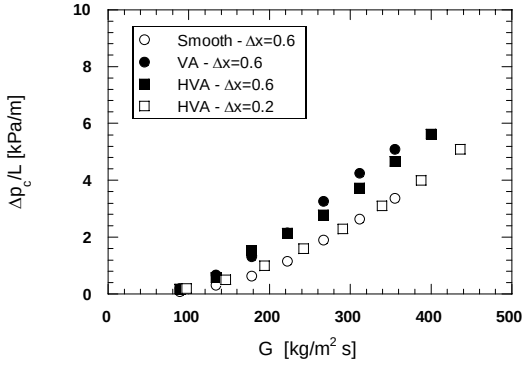

Figure 12. Condensation pressure drop $\Delta p_c/L$ versus mass flux G for fixed inlet quality x_{in} and quality change Δx.

microfin tubes at almost equal mass flux (242.3 and 222 kg/(m^{2}s)) and with Δx=0.2, it is seen that the rate of increase is much higher for the VA tube than for the HVA tube, confirming the above consideration; besides the HVA tube exhibits a behaviour quite similar to that, not shown, of the smooth tube. As for the influence of the quality change, data (not reported here) show that the heat transfer coefficient increases with increasing Δx. However, only moderate variations of heat transfer are displayed in the range of the tested quality change.

Attention will now be focused on pressure drop. Figures 9, 10 and 11 display data for the evaporation pressure drop, obtained in the same conditions reported in Figures 3, 5, and 6, respectively. For all tubes, pressure drop increases significantly with mass flux and quality. However, at higher vapour quality pressure drop falls off toward the data point for the only vapour phase pressure drop. Instead, the influence of quality change seems to be negligible, as can be seen from the inspection of Figure 11, which represents the variation of the pressure drop per unit length as a function of Δx for different mass fluxes G and fixed average quality x_m. As expected, the microfin tube displays pressure drops higher than those of the smooth tube, even if the increment is about 3.5 times at the most.

Condensation pressure drop for x_{in}=0.5 and x_{out}=0.3 is plotted versus mass flux and average quality in Figures 12 and 13 respectiveley. As for boiling, pressure drop is an increasing function of G and analogous considerations as for the behaviour of the condensation heat transfer coefficient hold; however, in contrast, the VA tube does not show an increase in pressure drop greater than that of the tube HVA. With reference to the effects of average quality, the experimental data show that at fixed mass flux and quality change (222 and 242.3 kg/(m^{2}s); Δx=0.3) pressure drop increases with average quality varying over the range between 0.2 and 0.8. Penalty factors, which are in fact the same for both the microfin tubes, range from 2 to 1.4.

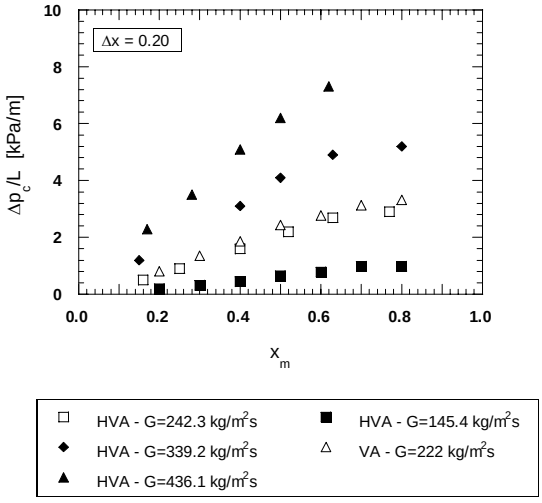

Figure 13. Condensation pressure drop $\Delta p_c/L$ versus average quality x_m for fixed mass flux G and quality change Δx.

4. CONCLUSIONS

In-tube evaporation and condensation heat transfer characteristics and pressure drop for R-134a inside two microfin tubes and a smooth tube are reported in this study. All the tubes have outer diameter of 9.52 mm and are horizontally operated. The two microfin tubes differ mainly in the number of fins, i.e., 54 in one case and 82 in the other one.

In the range of this study, both microfin tubes exhibit a significant heat transfer enhancement when compared to the smooth tube. Furthermore, microfins causes the onset of dryout to be shifted towards higher values of vapour quality because of their higher capability to keep the wall wet (liquid is conveyed upward).

Pressure drop also increases in the microfin tubes but to a less extent than heat transfer.

Tube VA, that is the tube with 54 fins, appears to

show the best heat transfer performance over the range of variables tested both in evaporation and condensation. Penalty factors are practically the same for both microfin tubes.

5. AKNOWLEDGEMENTS

This work is supported by MURST (the Italian Department for the University and for the Scientific and Technical Research) via COFIN 2004 grants.

The authors thank Alessandro Loschi and Roberto Locatelli for the aid in data collection.

REFERENCES

Cavallini A., Del Col B., Doretti L:, Longo G. A., Rossetto L. 2000, Condensation of refrigerants inside plain and enhanced tubes, *3rd European Thermal Sciences Conference 2000*, Vol. 1, pp. 51-60.

Cavallini A., Del Col B., Doretti L:, Longo G. A., Rossetto L. 1998, A new model for refrigerant vaporisation inside enhanced tubes, *3rd International Conference on Multiphase Flow, ICMF '98*, Lyon, France.

Chamra L. M., Tan M., Kung C. 2004, Evaluation of existing condensation heat transfer models in horizontal micro-fin tubes, *Experimental Thermal and Fluid Science*, 28, pp. 617-628, Elsevier.

Eckels S. J. and Pate M.B. 1992, Evaporation heat transfer coefficients for R-22 in micro-fin tubes of different configurations, *HTD*-Vol. 202, pp. 117-125.

Ito M. and Kimura H. 1979, Boiling heat transfer and pressure drop in internal spiral-grooved tubes, *Bulletin of JSME*, Vol. 2, No. 171, pp. 1251-1257.

Kandlikar S. G. and Raykoff T. 1996, Predicting flow boiling heat transfer for refrigerants in microfin tubes, *Proc. of 2nd European Thermal-Sciences and 14th UIT National Heat Transfer Conf.*, Vol. 1, pp. 475-482.

Muzzio A., Niro A. and Arosio S. 1998, Heat transfer and pressure drop during evaporation and condensation of R22 inside 9.52 mm O.D. microfin tubes of different geometries, *Enhanced Heat Transfer*, Vol. 5, pp. 39-52.

Schlager L. M. 1991, Boiling and condensation in microfin tubes, *VKI Lecture Series on Industrial Heat Exchangers*.

Thome J. R. 1994, Two-phase heat transfer to new refrigerants, *Heat transfer 1994, Proc. 10th Int'l Heat Transfer Conference*, Vol. 1, pp. 19-41.

Yasuda K., Ohizumi K., Hori M. and Kawamata O. 1990, Development of condensing thermofin-HEX-C tube, *Hi-tachi Cable Rev.*, 9, pp. 27-30.

Webb R. L. 1993, *Principles of enhanced heat transfer*, pp. 446-450, John Wiley & Sons, New York.

Webb R. L. 1994, Advances in modeling enhanced heat transfer surface, *Heat transfer 1994, Proc. 10th Int'l Heat Transfer Conference*, Vol. 1, pp. 445-459.